ACP
AMERICAN COLLEGE OF PROSTHODONTISTS®

Effect of Compromised Cortical Bone on Implant Load Distribution

Kıvanç Akça, DDS, PhD,[1,2] Mete I. Fanuscu, DDS,[3] & Angelo A. Caputo, PhD[4]

[1] Associate Professor, Department of Prosthodontics, Faculty of Dentistry, Hacettepe University, Ankara, Turkey
[2] Research Scholar, Division of Restorative Dentistry, School of Dentistry, University of California at Los Angeles, Los Angeles, CA
[3] Associate Clinical Professor, Division of Restorative Dentistry, School of Dentistry, University of California at Los Angeles, Los Angeles, CA
[4] Professor and Chairman, Biomaterials Science Section, Division of Advanced Prosthodontics, Biomaterials, and Hospital Dentistry, School of Dentistry, University of California at Los Angeles, Los Angeles, CA

Keywords
Biomechanics; implant design; bone–implant interface; peri-implantitis; overload.

Correspondence
Kıvanç Akça, Çetin Emeç Blv, 6. cadde, 54/3 06450 Öveçler, Ankara, Turkey. E-mail: akcak@hacettepe.edu.tr; kivanc.akca@superonline.com

Previously presented at the 15th European Association for Osseointegration (EAO) Congress, October 5 to 7, 2006, Zurich, Switzerland.

This study has been partly supported by The Scientific and Technical Research Council of Turkey, Directorate of Human Resources Development (TUBITAK-BAYG, NATO B2), Ankara, Turkey.

Accepted September 20, 2007

doi: 10.1111/j.1532-849X.2008.00365.x

Abstract

Purpose: To investigate photoelastically the difference in load distribution of dental implants with different implant neck designs in intact and compromised bone.
Materials and Methods: Composite photoelastic models were fabricated using two different resins to simulate trabecular bone and a 1-mm thick layer of cortical bone. The following parallel-sided, threaded implants were centrally located in individual models representing intact and compromised cortical bone: Straumann (4.1-mm diameter × 12-mm length), AstraTech (4.0-mm diameter × 13-mm length), and 3i (3.75-mm diameter × 13-mm length). The compromised cortical bone condition was simulated by contaminating a 1-mm neck portion with Vaseline to impair the implant–resin interface. Vertical and oblique static loads were applied on the abutments, and the resulting stresses were monitored photoelastically and recorded photograhphically.
Results: For the fully intact condition, the highest stresses were observed around the crest and apical region for all implant designs under vertical and inclined loads. There were no appreciable differences in magnitude or distribution between implant types. With compromised cortical bone, for all designs and load directions, higher stresses in the supporting structures were observed. Increased stresses were noted especially at the cortical bone–trabecular bone interface. Somewhat lower stress levels were observed with the 3i implant.
Conclusions: The condition of implant–cortical bone contact has considerable influence on stress distribution. A compromised cortical bone condition caused higher level stresses for all implant designs tested.

Marginal bone loss around dental implants supporting prostheses occurs to a certain level with dental implant systems.[1-5] Comparative clinical studies of different implant designs report similar levels of annual bone loss.[6-8] In a recent prospective cohort study,[9] different criteria widely used for the definition of success were compiled to evaluate 10-year success rates of titanium implants.[10-12] An implant with marginal annual bone loss of less than 0.2 mm following the first year of functional loading has been accepted as successful; however, disparity in reported bone loss around various implant systems, specifically in the first year of service, remains debatable.[10,13]

Experimental studies implicate peri-implantitis[14,15] and occlusal overload[16,17] as the primary causes leading to marginal bone loss. Initiation of this process remains unclear. In essence, biological and mechanical factors interact to set enviromental conditions before and after marginal bone reactions start taking place around dental implants at either the physiological or pathological level.

There are subsidiary factors claimed to be involved in marginal bone level changes.[9] In regard to mechanical factors, implant macrogeometry's impact on marginal bone level changes has been studied. Accordingly, the bone loss for single-tooth Brånemark implants with a conical collar design demonstrated a significantly greater amount of bone loss than Brånemark self-tapping implants.[18] In part, increased marginal bone loss with a nonthreaded conical neck design is likely to be consistent with the lack of retention element at implant collar.[19] This hypothesis may be correct due to extremely stable marginal bone level found around AstraTech implants using a microthread configuration at the implant neck.[20] On the contrary, in a randomized clinical study,[21] acid-etched/sandblasted Straumann dental implants with no thread configuration at the marginal bone level also displayed comparable bone stability. Thus, the effect of geometrical specifications at the implant neck on load distribution in marginal bone is not sufficiently known.

In addition, load transfer around an implant with compromised marginal bone conditions would be further complicated in the presence of inflammatory bacterial infiltration. Therefore, understanding the biomechanical consequences of impairment at the bone–implant interface, specifically at early stages, is quite crucial; however, thus far, in vitro studies dealing with this issue are very limited. Therefore, the objective of this research was to evaluate the effect of implant neck designs in simulated intact and compromised cortical bone conditions on load transfer using photoelastic stress analysis.

Materials and methods

This in vitro biomechanical study included Straumann (Ø 4.1-mm diameter × 12-mm length, Institut Straumann, Basel, Switzerland), AstraTech (Ø 4.0-mm diameter × 13-mm length, AstraTech AB, Mölndal, Sweden), and 3i (Ø 3.75-mm diameter × 13-mm length, Implant Innovations, Inc., A Biomet Company, Palm Beach Gardens, FL) dental implants for comparative evaluation of various implant neck designs (Fig 1). Surfaces of the Straumann, AstraTech, and 3i dental implants were sandblasted/acid-etched, TiO_2 grit-blasted, and machined, respectively.

For quasi-3D photoelastic stress analysis, each implant design was included in two photoelastic models to simulate intact and compromised cortical bone conditions. Experimental models were fabricated using individual simulants with different stiffnesses to approximate the ratio of elastic moduli between cortical and trabecular bone. PL-2 (Measurements Group, Inc., Raleigh, NC) was used to represent trabecular bone with a layer of 1-mm thick PLM-1 (Measurements Group, Inc.) as cortical bone.[22]

For fabrication of experimental models, a master mold was obtained from a 40 × 40 × 40-mm^3 aluminum block (EN-AW-AlMg1SiCu) using silicone impression material (Dow Corning 3110 RTV, Dow Corning, Midland, MI). With the same procedure, a subsidiary mold was made to fabricate a 1-mm cortical bone layer. In the fabrication of a model with intact cortical

Figure 1 Dental implant designs used in the study (l to r, Straumann; 3i, AstraTech).

Figure 2 Completed composite model holding vertically placed dental implant.

bone, a dental implant was centrally located into the subsidiary mold with the long axis perpendicular to the top surface of the mold. PLM-1 mixture was prepared according to the recommendations of the manufacturer, and was injected to fabricate cortical bone simulant. Upon completion of polymerization, the photoelastic cortical bone model attached to the implant was removed from the mold. The lower surface of the resin was roughened with abrasive papers to enhance micromechanical attachment with the trabecular bone simulant. Then, the cortical bone simulant holding the implant was placed into the master mold to incorporate trabecular bone. PL-2 was cast into the impression directly around the implant and allowed to cure sufficiently (Fig 2).

In fabrication of a model with compromised cortical bone, debonding of the bone–implant interface at the marginal bone level was simulated. For this purpose, prior to fabrication of cortical bone simulant, a 1-mm implant neck portion was contaminated with circular treatment of Vaseline using an applicator tip (Dentsply, DeTrey GmbH, Konstanz, Germany). Then, the above-described procedures for model fabrication with intact cortical bone were followed using the contaminated implant. A total of 12 composite models, six each for intact and compromised cortical bone conditions, were completed to photoelastically visualize peri-implant stresses developed under experimental loading conditions.

To standardize the distance from the upper surface of the models to the applied load level (≅9 mm), solid abutment (048.541, Institut Straumann), direct abutment 5 high (240007, AstraTech AB), and GingHue Post (APP452g, 3i Implant Innovations) were selected and were torque-tightened into the implants with 35, 25, and 32 Ncm, respectively. Prior to experimental loadings, models were confirmed to be stress-free. Vertical and oblique (20° angle) static occlusal loads of 10, 20, and 30 lb were applied in sequence on top of the abutments. Load was applied in a loading frame by means of a calibrated load cell mounted on the movable head of the frame. Forces were monitored and controlled by a digital read-out after signal treatment using a strain gauge conditioner (models 2130

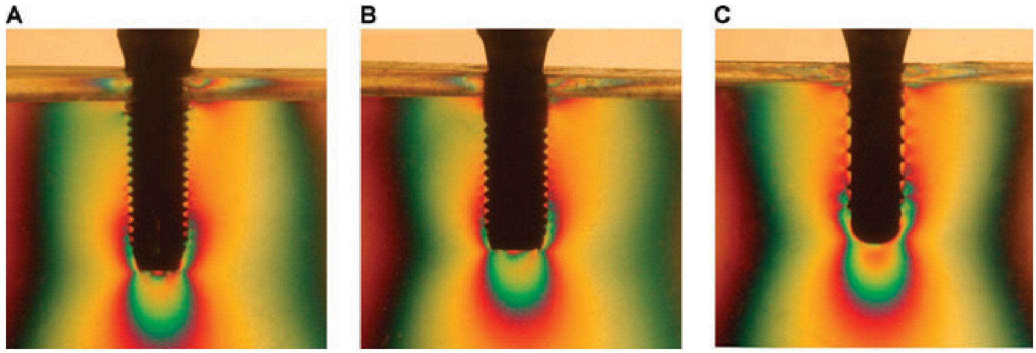

Figure 3 Stresses developed under 30-lb vertical load in intact models with (A) 3i dental implant, (B) AstraTech dental implant, and (C) Straumann dental implant.

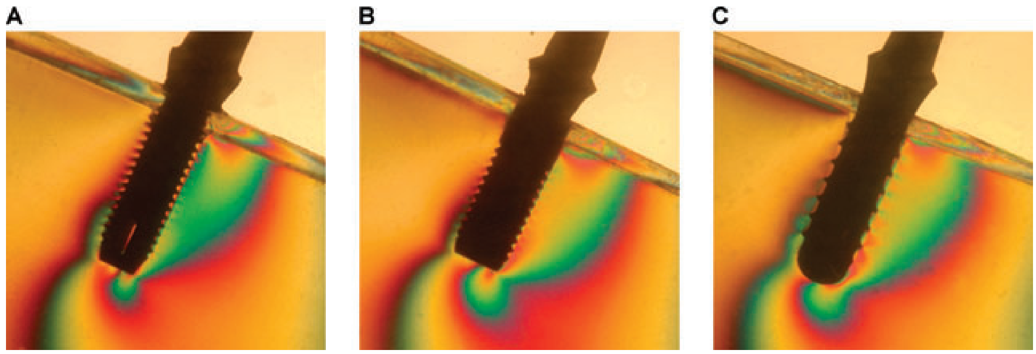

Figure 4 Stresses produced under 30-lb oblique load in intact models with (A) 3i dental implant, (B) AstraTech dental implant, and (C) Straumann dental implant.

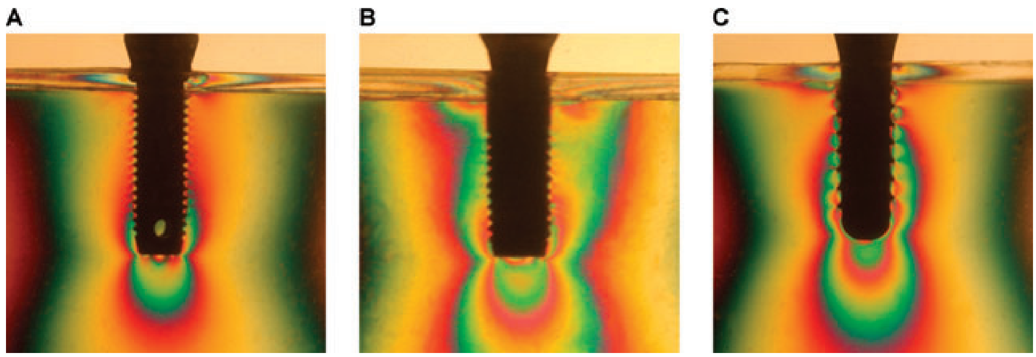

Figure 5 Increased stress intensity particularly in trabecular bone around (A) 3i dental implant, (B) AstraTech dental implant, and (C) Straumann dental implant in compromised models in comparison to intact models under vertical load.

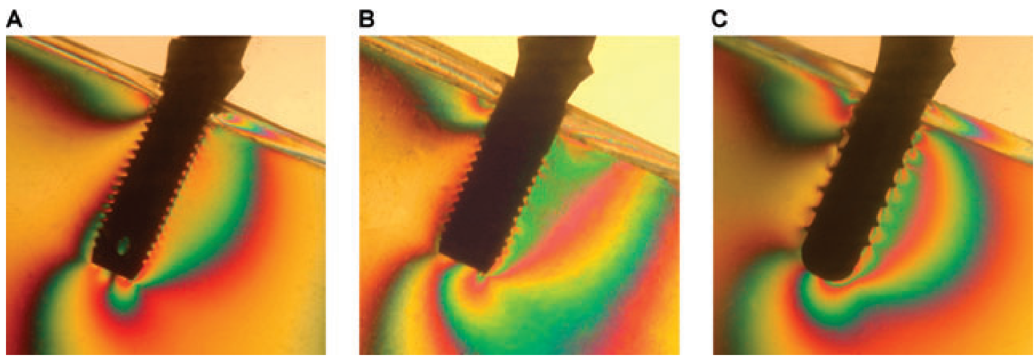

Figure 6 Stress concentration observed in the tension side at the interface of the trabecular and cortical simulants at the neck of (A) 3i dental implant, (B) AstraTech dental implant, and (C) Straumann dental implant in compromised models.

and 2120A, Instruments Division, Measurements Group, Inc.). During loading, the models were placed in a tank of mineral oil to minimize surface refraction and facilitate photoelastic observation. The stresses that developed in the supporting structures were observed and recorded photographically in the field of a circular polariscope (Measurements Group, Inc.). Photoelastic stress fringes were analyzed and interpreted as described previously.[23,24]

Results

For all implant neck designs tested, the stresses developed were proportional to the applied load level. To facilitate presentation, only the results for the 30-lb load will be given below.

Models with intact cortical bone

Under axial loading of all implants, stresses were localized at the implant apex, within the cortical simulant at the neck, and at the interface of the trabecular and cortical simulants at the neck (Fig 3). Although the general distribution of load-induced stress was similar, some differences were noted. For example, the intensity of stress at the above locations tended to be somewhat higher with the Straumann design than the AstraTech and 3i neck designs. Load transfer was evident at the threads for all designs, with more distinct localizations around the Straumann design, which has fewer threads.

Under oblique loading of all implants, stresses again were localized at the implant apex, within the cortical simulant at the neck, and at the interface of the trabecular and cortical simulants at the neck (Fig 4); however, in contrast with the axial load, a nonsymmetric distribution developed. Stresses for each implant were localized on the compression side, the side opposite the location of force application. The highest stresses at this location in the cortical simulant and at the cortical-trabecular simulants were seen with the Straumann and Astra implants. Stresses at the apex of these implants also were slightly higher than the 3i implant. Overall, the 3i implant was less stressful to the supporting structures.

Models with compromised cortical bone

Under axial loading of all implants, although stress localizations were the same as observed around the implants with intact cortical bone, differences in stress distribution and intensity were remarkable. Basically, the trabecular bone simulant was placed under more concentrated and higher stresses for all implant designs tested in comparison to models with intact cortical bone (Fig 5). More importantly, load-induced stresses in trabecular bone simulant notably differed between implant designs. Increase in load transfer along the implant threads of Straumann and Astra implants was discernable. In addition, stress intensity and concentration at cortical–trabecular bone interface were the highest with Astra neck design.

Under oblique loading of all implants, stress localizations were the same as observed around the implants with intact cortical bone. In comparison to intact cortical bone, stress distribution was similar at the implant apex and within the cortical simulant at the neck; however, in contrast to models with intact cortical bone, stress concentration was also observed on the tension side, the side of force application, at the interface of the trabecular, and cortical simulants at the neck (Fig 6). Additionally, stresses were notably higher than of those observed in models with intact cortical bone for all implants tested. Differences between load-induced stresses around the implant designs were evident. Straumann and Astra implants displayed similar but higher stresses than the 3i implant at the apex, within the cortical simulant at the neck, and at the interface of the trabecular and cortical simulants at the neck.

Discussion

Photoelastic analysis is a unique technique to visualize full-field stress distribution resulting from interference of components of polarized light when transmitted by an experimentally loaded plastic model. Photoelastic methods have been applied to investigate biomechanical behavior of dental implants in bone supporting fixed and removable prostheses;[25-27] however, representing the nonhomogeneous and anisotropic structure of bone by plastic models gives rise to certain limitations in predictions of biological response to applied loads. Nevertheless, photoelastic models have successfully indicated differences between various conditions by comparative evaluation of stress-related outcomes.

As in many other biomechanical studies, the gap between the information obtained at in vitro and in vivo levels could be bridged by establishing more realistic experimental conditions. For this purpose, composite modeling employing concurrent simulation of cortical and trabecular bone has been introduced recently to form more effective photoelastic models. These models facilitate explanation of perplexing bone conditions.[22,23] Although the elastic moduli of the bone simulants depart from actual values of cortical and trabecular bone, the ratio of elastic moduli between cortical and trabecular bone simulants (PLM-1 and PL-2, respectively) falls into a realistic range.[22] In this study, cortical and trabecular bones were separately simulated to fabricate more realistic photoelastic models to reflect the early stages of a compromised bone–implant interface.

The impact on load distribution of a peri-implant defect around the implant neck has been studied photoelastically.[22] In essence, deterioration in the bone–implant interface is likely to start before concrete bone resorption occurs. In the current study, compromise in bone-to-implant contact at the cortical bone level was simulated by contamination of the implant surface to interfere, and consequently lead to poor mechanical retention with the bone simulant. The outcomes revealed that characterization of stress intensity and concentration at cortical and trabecular bone simulants after contamination differed considerably under vertical and oblique load conditions. Therefore, the method followed to simulate compromised cortical bone may be acceptable at least in terms of establishing the difference from intact cortical bone.

The biomechanical relationship between the implant neck and surrounding bone has been considered to have an important influence on the success of implant-supported restorations. Accordingly, various implant designs presenting different implant–abutment connections have been introduced to create stable marginal bone levels with a minimum amount of bone loss. In the present study, the 3i dental implant neck design tended to present slightly lower stress levels than AstraTech and Straumann dental implants both in intact and compromised cortical bone under loading conditons. The photoelastic analysis has limited potential to distinguish the differences in detail. In this regard, refinement of the results with regards to implant designs that do not present dramatic change in load distribution will be questionable; however, the stress intensity and concentration in compromised cortical bone condition was remarkably different than those established in intact bone conditions for the three tested implant designs. The major difference was the stress concentration on the side of force application at the interface of the trabecular and cortical simulants. This clearly indicates that the compromise in bone–implant interface remarkably alters the peri-implant load distribution regardless of the implant design. Therefore, peri-implant bone condition may have a prevailing effect over implant design on load distribution around an implant. Biomechanical studies are required to substantiate the above premise.

Conclusions

Within the limitation of this biomechanical study, the condition of implant–cortical bone contact has considerable influence on stress distribution. Compromised cortical bone caused higher stress levels for all implant designs tested, with a smaller effect noted with the 3i implant.

References

1. Buser D, Mericske-Stern R, Bernard JP, et al: Long term evaluation of non-submerged ITI implants. Part 1: 8-year life table analysis of a prospective multi-center study with 2359 implants. Clin Oral Implants Res 1997;8:161-172
2. Attard NJ, Zarb GA: Long-term treatment outcomes in edentulous patients with implant-fixed prostheses: the Toronto study. Int J Prosthodont 2004;17:417-424
3. Gotfredsen K, Holm B: Implant-supported mandibular overdentures retained with ball or bar attachements: a randomized prospective 5-year study. Int J Prosthodont 2000;13:125-130
4. Davarpanah M, Martinez H, Etienne D, et al: A prospective multicenter evaluation of 1,583 3i implants: 1- to 5-year data. Int J Oral Maxillofac Implants 2002;17:820-828
5. Ricci G, Aimetti M, Stablum W, et al: Crestal bone resorption 5 years after implant loading: clinical and radiologic results with a 2-stage implant system. Int J Oral Maxillofac Implants 2004;19:597-602
6. Moberg LE, Kondell PA, Sagulin GB, et al: Brånemark system and ITI dental implant system for treatment of mandibular edentulism. A comparative randomized study: 3-year follow-up. Clin Oral Implants Res 2001;12:450-461
7. Åstrand P, Engquist B, Dahlgren S, et al: Astra Tech and Brånemark System implants: a prospective 5-year comparative study. Results after one year. Clin Implant Dent Related Res 1999;1:17-26
8. Meijer HJ, Batenburg RH, Raghoebar GM, et al: Mandibular overdentures supported by two Brånemark, IMZ or ITI implants: a 5-year prospective study. J Clin Periodontol 2004;31:522-526
9. Karoussis IK, Bragger U, Salvi GE, et al: Effect of implant design on survival and success rates of titanium oral implants: a 10-year prospective cohort study of the ITI Dental Implant System. Clin Oral Implants Res 2004;15:8-17
10. Albrektsson T, Zarb G, Worthinton P, et al: The long term efficacy of currently used dental implants: a review and proposed criteria of success. Int J Oral Maxillofac Implants 1986;1:11-25
11. Buser D, Weber HP, Lang NP: Tissue integration of non-submerged implants. 1-year results of a prospective study with 100 ITI hollow-cylinder and hollow-screw implants. Clin Oral Implants Res 1990;1:33-40
12. Mombelli A, Lang NP: Clinical parameters for the evaluation of dental implants. Periodontol 1994;4:81-86
13. Weber HP, Crohin CC, Fiorellini JP: A 5-year prospective clinical and radiographic study of non-submerged dental implants. Clin Oral Implants Res 2000;11:144-153
14. Lindhe J, Berglundh T, Ericsson I, et al: Experimental breakdown of peri-implant and periodontal tissues. Clin Oral Implants Res 1992;3:9-16
15. Lang NP, Brägger U, Walther D, et al: Ligature-induced periimplant infection in cynomolgus monkeys. I. Clinical and radiographic findings. Clin Oral Implants Res 1993;4:2-11
16. Isidor F: Loss of osseointegration caused by occlusal load of oral implants. A clinical and radiographic study in monkeys. Clin Oral Implants Res 1996;7:143-152
17. Miyata T, Kobayashi Y, Araki H, et al: The influence of controlled occlusal overload on peri-implant tissue. Part 3: a histologic study in monkeys. Int J Oral Maxillofac Implants 2000;15:425-431
18. Quirynen M, Naert I, van Steenberghe D: Fixture design and overload influence marginal bone loss and fixture success of the Brånemark system®. Clin Oral Implants Res 1992;3: 104-111
19. Hansson S: The implant neck: smooth or provided with retention elements. A biomechanical approach. Clin Oral Implants Res 1999;10:394-405
20. Palmer RM, Smith BJ, Palmer PJ, et al: A prospective study of Astra single tooth implants. Clin Oral Implants Res 1997;8: 173-179
21. Galvi G, Gallini G, Lang NP: Early loading (2 or 6 weeks) of sandblasted and acid-etched (SLA) ITI implants in the posterior mandible. A 1-year randomized controlled clinical trial. Clin Oral Implants Res 2004;15:142-149
22. Jeong CM, Caputo AA, Wylie RS, et al: Bicortically stabilized implant load transfer. Int J Oral Maxillofac Implants 2003;18:59-65
23. Fanuscu MI, Caputo AA: Load transfer by an implant in a sinus-grafted maxillary model. J Prosthodont 2004;13:214-220
24. Cehreli M, Duyck J, De cooman M, et al: Implants design and interface force transfer. A Photoelastic and strain-gauge analysis. Clin Oral Implants Res 2004;15:249-257
25. Guichet D, Yoshinobu D, Caputo AA: Effect of splinting and interproximal contact tightness on load transfer by implant restorations. J Prosthet Dent 2002;87:528-535
26. Sadowsky SJ, Caputo AA: Stress transfer of four mandibular implant overdenture cantilever designs. J Prosthet Dent 2004;92:328-336
27. Itoh H, Caputo AA, Kuroe T, et al: Biomechanical comparison of straight and staggered implant placement configurations. Int J Periodontics Restorative Dent 2004;24:47-55